Preparation and characterisation of a novel fire retardant PET/α-zirconium phosphate nanocomposite

De-Yi Wang[a], Xue-Qi Liu[a], Jun-Sheng Wang[a], Yu-Zhong Wang [a][*], Anna A. Stec[b], and

T. Richard Hull[b][*]

a Center for Degradable and Flame-Retardant Polymeric Materials, College of Chemistry, Sichuan University, Chengdu 610064, China
b Centre for Fire and Hazards Science, School of Forensic and Investigative Science, University of Central Lancashire, Preston PR1 2HE, UK

Abstract:

The preparation of a novel fire retardant nanocomposite of poly (ethylene terephthalate) (PET)/α-zirconium phosphate (α-ZrP) by in situ polymerization was investigated. The novel fire retarded PET nanocomposite, PET-co-DDP/α-ZrP nanocomposite, was synthesized by the direct condensation of terephthalic acid, ethylene glycol, 9,10-dihydro-10[2,3-di(hydroxycarbonyl)propyl]-10-phosphaphenanthrene-10-oxide and nano α-ZrP. The morphology，thermal stability and burning behaviour of the nanocomposite with 1 wt-% α-ZrP loadings were investigated. The extent of dispersion of the nanofillers was quantified by X-ray diffraction, scanning electron microscopy and transmission electron microscopy. Significant improvements in fire retardant performance were observed for the nanocomposite from limiting oxygen index (increased from 21.2 to 32.6), UL-94 (achieving V-0), and cone calorimetry (reducing both the heat release rate and the total heat released, without reducing the time to ignition).

Key words: Fire retardant; flame retarded; poly(ethylene terephthalate); PET; *In situ*

---

[*] Corresponding author. Tel. & Fax: +86-28-85410259; *E-mail:* yzwang@email.scu.edu.cn (Y. -Z. Wang)

[*] Corresponding author. Tel: +44 (0)1772893543; fax: +44 (0)1772894981. *E-mail*：trhull@uclan.ac.uk(T.R. Hull).

1

polymerisation; nanocomposite; cone calorimeter, zirconium phosphate

1. Introduction

Poly (ethylene terephthalate) (PET) is a semicrystalline polymer possessing excellent chemical resistance, thermal stability, high strength, and spinnability. PET fibre is the textile industry's most widely used synthetic [1-3]. However, its flammability and severe dripping during combustion greatly limits its applications. As a result of recent studies of fire retarded PET, phosphorus-containing copolyesters have been recognized as one of the most efficient ways of imparting fire retardance to PET, because they have excellent fire retardancy and compared to halogenated flame retardants, lower toxic gas evolution during burning. Asrar and Mo [4] studied the synthesis of a copolyester, PET-co-CEPP, from terephthalic acid (TPA), ethylene glycol (EG) and 2-carboyethyl (phenylphosphinic) acid (CEPP). War et al [5-8] have also synthesized some novel phosphorus-containing fire retardants in polyester copolymers. Recently our laboratory in Chengdu has successfully synthesized a series of phosphorus-containing fire retardant polyesters copolymers including those with phosphorus linked as pendent groups and incorporated into the main chain [9-16]. Furthermore, it has also been noticed by various groups that the formation of nanocomposites can improve the fire retardant performance at relatively low nanoparticle loadings [17, 18, 19].

Polymer nanocomposites containing layered silicates have been studied extensively as a new generation of advanced composites that exhibit greatly improved mechanical properties [20], enhanced gas barrier properties [21], and fire retardancy [17]. Among the layered nanofillers, montmorillonite (MMT) clay is one of the most widely used nanofiller for preparing polymer nanocomposites due to its high ion exchange capacity for attachment of surfactant molecules, and high aspect ratio for better barrier properties. [20]. Zirconium bis(monohydrogen orthophosphate) monohydrate, $(\alpha\text{-}Zr(HPO_4)_2\cdot H_2O)$ $(\alpha\text{-}ZrP)$, is a layered structure material with many interesting features, such as high ion-exchange capacity, thermal and chemical stability [22],

catalytic activity, ionic conductivity, and the potential to delaminate and become intercalated within the polymer [23]. Many of these properties are common to natural layered nanofillers such as montmorillonite, but α-ZrP has a higher ion exchange capacity [24], and has different elements in its structure. However, only a few studies have been reported on layered zirconium phosphate polymer nanocomposites, such as preparation of epoxy-α-ZrP [24-27] nanocomposites, polyethyleneimine-γ-ZrP nanocomposites [28] and poly (ethylene terephthalate)/lamellar zirconium phosphate nanocomposites [23]. Furthermore, the foci of these studies was the synthesis and the improvement of thermal or mechanical properties. To the best of our knowledge, no studies of fire retardant property enhancement by ZrP have been reported, although its structure contains elements (zirconium and phosphorus) with potential fire retardant properties.

In this work, we describe the preparation of a novel fire retarded PET nanocomposite with α-ZrP by *in situ* polymerization. α-ZrP was synthesized by direct precipitation. The PET nanocomposite, PET-co-DDP/zirconium phosphate (α-ZrP) nanocomposite, was synthesized by condensation of terephthalic acid (TPA), ethylene glycol (EG), 9, 10 - dihydro-10 [2,3-di(hydroxycarbonyl)propyl] -10-phosphaphenen-threne- 10- oxide (DDP) and nano-ZrP as shown in scheme 1. The thermal stability and burning behaviour of the nanocomposite has been investigated and are presented here.
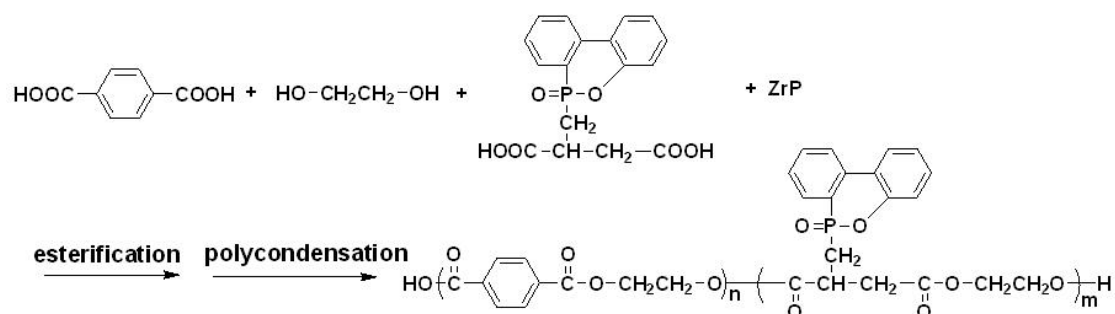
Scheme 1 Reaction route of PET-co-DDP/ZrP nanocomposite

2. Experimental

2.1 Materials

TPA and EG were supplied by Zhenghao New Materials Company (Jinan, China). α-ZrP was synthesized in our laboratory in Chengdu from zirconium oxychloride ($ZrOCl_2$) and phosphoric acid (H_3PO_4) both from the Shanghai Chemical Agent Company, and modified using diethanolamine (($HOCH_2CH_2)_2NH$) and octadecyltrimethylammonium chloride (1831) through cation exchange. DDP was provided by Weili Flame Retardant Chemicals Industry Co. Ltd. (Chengdu, China).

2.2 Preparation and modification of α-ZrP

α-ZrP was synthesized from $ZrOCl_2$ and H_3PO_4, having established that the optimum synthesis condition was achieved when the mole ratio of $ZrOCl_2$ to H_3PO_4 was 1:2 and the mixture reacted for 8 hours at 40^oC. The precipitate was filtered and washed using de-ionised water until the rinsing water was neutral (pH 7). The results from XRD concur with those of reference 27. The layered structure of α-ZrP was modified by two routes using ($HOCH_2CH_2)_2NH$ and 1831, by cation exchange under various conditions. For the first modification, the optimum conditions was obtained when the mole ratio of ($HOCH_2CH_2)_2NH$ and α-ZrP was 2.5 and the exchange time was 10 hours at 40°C with stirring. The product was washed with deionised water until the washing water was neutral. This was further modified with 1831 and the ($HOCH_2CH_2)_2NH$-modified α-ZrP in a 2.5 mole ratio using an exchange time of 12 hours at 60°C with stirring. This modified ZrP was centrifuged and washed with deionised water until neutral.

2.3 Preparation of PET-co-DDP/α-ZrP nanocomposites

PET-co-DDP/α-ZrP nanocomposite was prepared from TPA, EG, DDP and modified α-ZrP by direct condensation polymerisation. The synthetic route was as follows: initially, the modified α-ZrP (1wt %) was added to EG (200 ml) and stirred

in an ultrasonic bath for 0.5 hour as pretreatment. After this, TPA, EG, DDP and the pretreated α-ZrP solutions were introduced into a reactor equipped with a nitrogen inlet, a condenser and a mechanical stirrer. The reactor was heated to 240ºC under high pressure (0.4-0.5MPa) and maintained for 3.5 h. After this, the pressure of the reactor was reduced to less than 100 Pa and maintained for 2 h. A comparison material, PET-co-DDP with 1wt% phosphorous was prepared from TPA, EG and DDP according to the procedure reported by Chang et al. [29]. The intrinsic viscosities (η) of the copolyesters were determined with an Ubbelohde viscometer at 30ºC in phenol / 1,1,2,2 - tetrachloroethane (60/40, w/w) solution; the results are given in Table 1.

Sample	P % (w/w)	ZrP % (w/w)	[η] (dl /g)	LOI	UL-94	Drip
PET	0	0	0.67	21.2	No rating	severe
PET-co-DDP	1	0	0.65	30.8	V-2	moderate
PET-co-DDP/ZrP nanocomposite	1	1	0.64	32.6	V-0	show

Table 1 Summary of copolyester characterisation.

2.4. Characterization

2.4.1 X-ray diffraction (XRD)

X-ray diffraction (XRD) was performed using a Rigaku X-ray powder diffracttometer with a copper target. The generator power was 40 kV and 150 mA, the scan mode was continuous with a scan rate of 0.8°/min, and the 2θ scan range was from 2° to 45°.

2.4.2 Scanning electron microscopy (SEM)

PET-co-DDP/α-ZrP nanocomposite was made into films and then cracked in liquid N_2. The fresh face of the sample was gold coated for SEM observation. The sample was examined in a JEOL JSM-5410 scanning electron microscope (Tokyo, Japan) using a working voltage of 10 kV.

2.4.3 Transmission electronic microscopy (TEM)

TEM images of nanocomposite specimens without staining were taken at room temperature. The TEM grids were mounted in a liquid nitrogen cooled sample holder. The ultrathin sectioning (50–70 nm) was performed by ultramicrotomy at low temperature using a Reichert Ultracut E low temperature sectioning system. A transmission electron microscope (JEM-100CX, JEOL) operated at 80kV was used to obtain images of the nanocomposite specimens.

2.4.4. LOI and UL-94 test

The LOI values were measured on a JF-3 oxygen index meter (Jiangning, China) with sheet dimensions of 130×6.5×3 mm^3 according to ASTM D2863-97. Vertical burning tests (UL-94) were conducted on a vertical burning test instrument (CZF-2-type) (Jiangning, China) with sheet dimensions of 130×13×3 mm^3 according to ASTM D3801.

2.4.5. Thermogravimetric analysis (TGA)

Thermogravimetric analysis (TGA) was performed on a DuPont 1090B thermogravimetric analyzer at a heating rate of 10 ^{o}C/min. 10 mg of samples were examined under flowing air (60ml/min) over a temperature range from room temperature to 700 ^{o}C.

2.4.6. Cone calorimetry [33]

The cone calorimeter tests were carried out following the procedures indicated in the ISO 5660 standard with a FTT cone calorimeter. Square specimens (100×100×6 mm^3) were irradiated at a heat flux of 50 kW/m^2.

3. Results and discussion

3.1 Structure and morphology

The structure and morphology of the nanocomposite has been investigated by the XRD, SEM and TEM. It is known that ZrP has a clay-like layered structure, which

can be characterised using XRD, and the distance of between layers calculated from the Bragg equation. Fig. 1 (a), (b), (c) and (d) presents, the XRD results of ZrP, modified ZrP using $(HOCH_2CH_2)_2NH$ and 1831 and PET-co-DDP/ZrP nanocomposite respectively. From fig. 1, it can be seen that the first peak of the ZrP shifts to a low angle after modification indicating greater separation of the ZrP layers, with some of the ZrP layers being further separated on modification. On formation of a nanocomposite, the layering from the lack of peak at $2\theta = 11°$ and shifted to 8° and 6° becomes indistinct, suggesting partial to complete exfoliation. Inputing the 2θ values into the Bragg equation suggests increases in the interlayer separation from 0.77 nm to 1.13 nm and 1.52 nm by the incorporation of the modifier molecules. Finally after polymerisation and nanocomposite formation the interlayer distance is further increased from 1.52 nm to 2.38 nm. These results show the nanocomposite has been formed, and the nanofillers is well-dispersed. Further evidence is seen in SEM and TEM as shown in fig. 2 and fig. 3. From fig. 2, layered structures with plate-like appearance are evident, and these show good dispersion. The internal structures of the nanocomposites in the nanometre scale were observed by TEM and are shown in fig. 3; the dark entities are the cross sections of intercalated ZrP layers. Stacked ZrP monolayers can be seen (arrowed) in the copolymer matrix. From these results, it can be concluded that PET-co-DDP/α-ZrP nanocomposite has been adequately dispersed.
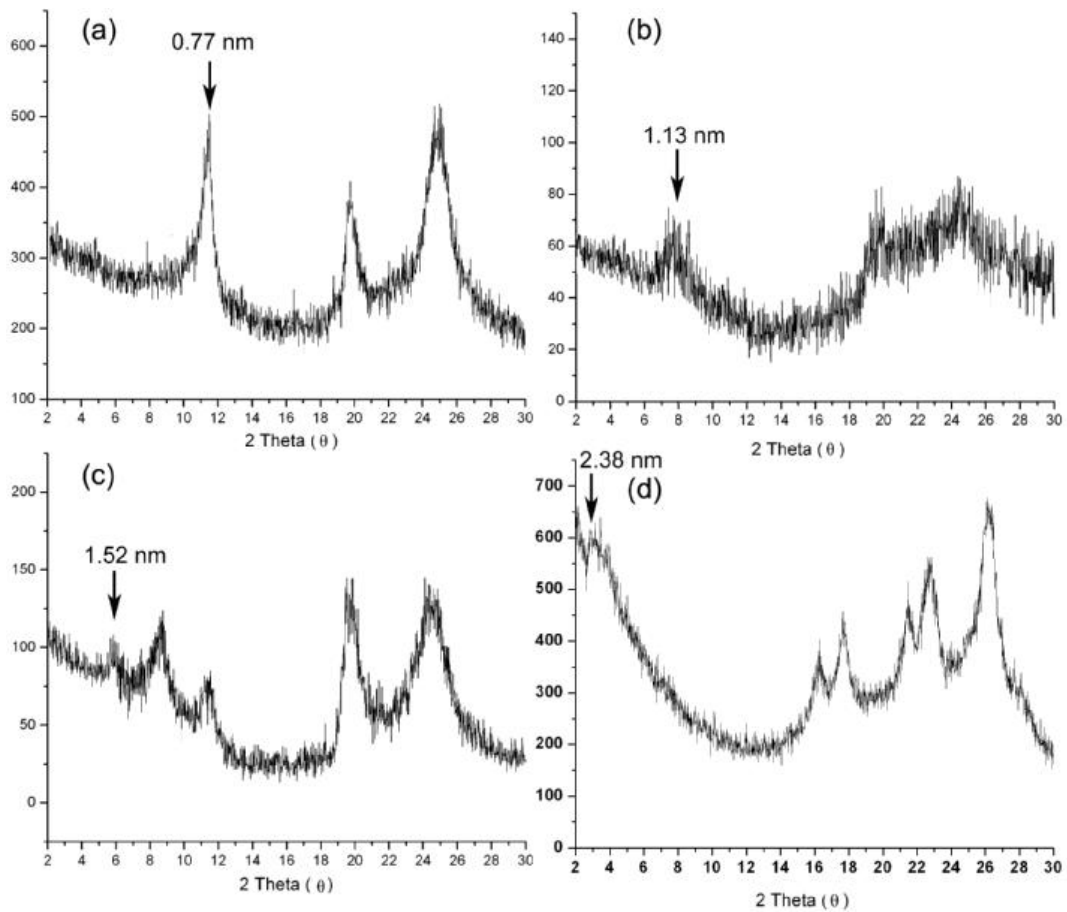
Fig. 1. XRD results: (**a**) ZrP (**b**) ZrP modified by (HOCH$_2$CH$_2$)$_2$NH (**c**) ZrP modified twice (**d**) PET-co-DDP/ZrP nanocomposite
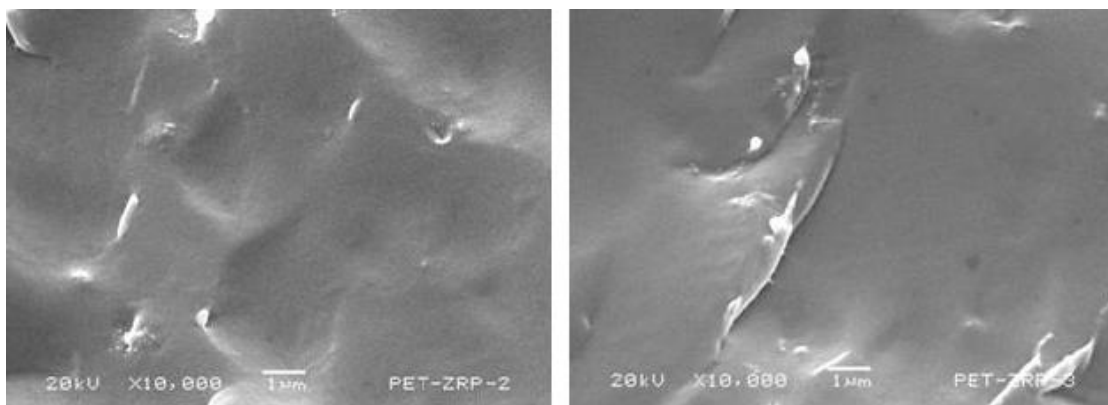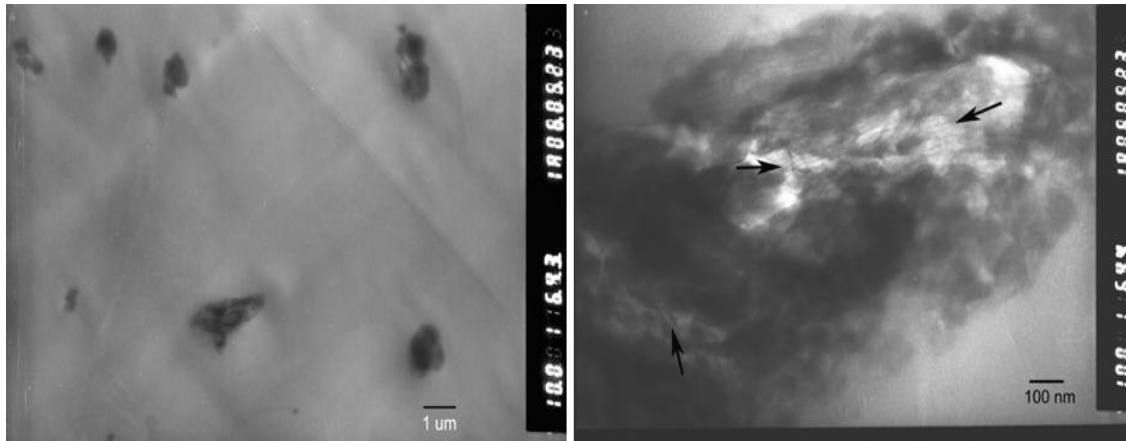

Fig. 2 SEM for the PET-co-DDP/ZrP nanocomposite

Fig. 3. TEM for the PET-co-DDP/ZrP nanocomposite

3.2. Thermal stability

In order to understand the thermal stability of the PET-co-DDP/α-ZrP nanocomposite, the thermal degradation behaviour for the various samples was compared. TGA testing of PET, PET-co-DDP and PET-co-DDP/α-ZrP nanocomposite was carried out in air at a heating rate 10 $^{\circ}$C /min. TG curves are presented in figure 4, and some detailed data is shown in table 2. Ignition of a polymer can occur when a critical fuel air ratio is reached in the gas phase, such that its heat of combustion provides sufficient heat for its replacement. Thus any reduction in fuel production rate around 5 – 10% mass loss is likely to increase the time to ignition. From the figure and table a significant difference is seen when comparing the initial decomposition temperature (T_{onset}) of PET, PET-co-DDP and PET-co-DDP/α-ZrP nanocomposite; T_{onset} has been increased from 375°C to 401°C and 411°C, quantifying the improvement in the thermal stability of the PET; $T_{50\%}$ shows a similar but smaller trend. In addition, the char yield of the copolymer and nanocomposite increase when compared to pure PET. This may result from the phosphorus in DDP forming phosphoric acid and promoting carbonization on the surface of polymer. As char forms a barrier, preventing heat and fuel transfer between the flame zone and the underlying substrate, additional char formation would be expected to protect the substrate from heat and improve the fire retardant performance.
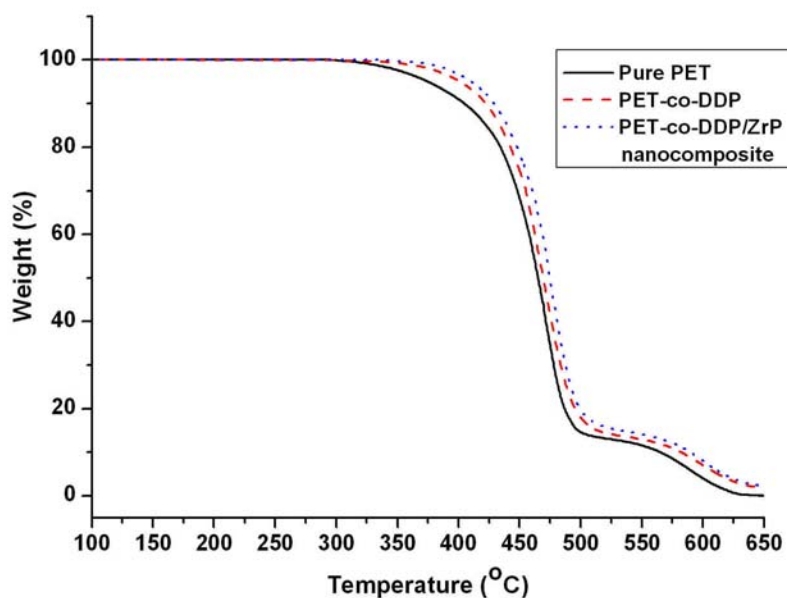
Fig.4 the TG results for samples studied

sample	T_{onset}^{a}(℃)	$T_{50\%}^{b}$(℃)	Y_{600}^{c}(%)	Y_{650}^{d}(%)
PET	375	465	3.98	0.05
PET-co-DDP	401	469	7.00	1.84
PET-co-DDP/α-ZrP nanocomposite	411	475	8.10	2.21

a) T_{onset} − the onset degradation temperature (temperature at 5% mass loss).

b) $T_{50\%}$ − the temperature at 50% mass loss.

c) Y_{600} − the yield of residue at 600°C.

d) Y_{650} − the yield of residue at 650°C.

Table 2 The results from TG curves of various samples (heating rate: 10℃/min in air)

3.3. Burning behaviour

3.3.1. Small flame tests

Limiting oxygen index (LOI) and Bunsen burner tests such as the UL-94 are widely used to evaluate fire retardant formulations. The LOI and UL-94 classification of each sample was determined, as shown in table 1. It can be observed that the LOI value of PET increased from 21.2 to 30.8 when 1 wt% P was

present in the copolymer, and the UL-94 reached V-2, due to flaming drips. However, the PET-co-DDP/α-ZrP nanocomposite gave an LOI of 32.6, and a UL-94 rating of V-0, with a total nanoparticle content of only 1%. This may be due to an increase in the melt viscosity near the ignition temperature, reducing the dripping tendency as a result of the presence of a well-dispersed nanofiller. Meanwhile, the metal in the nanoparticle may have catalyzed the carbonization of the polymer forming a more effective char layer, reducing the transfer of heat and fuel.

3.3.2. Cone calorimetry

The cone calorimeter is a bench-scale fire test apparatus and provides a wealth of information on combustion behaviour [30]. Some cone calorimeter results have been found to correlate well with those obtained from large scale fire tests, so that it can be used to predict the behaviour of materials in a real fire [31]. It is a useful tool for the evaluation of fire retardant materials and quantifies fire parameters such as time to ignition (TTI), heat release rate (HRR), and total heat release (THR). Figure 5 shows curves of the heat release rate (HRR) against time of pure PET, PET-co-DDP and PET-co-DDP/ZrP nanocomposite. Pure PET burns rapidly after ignition and a sharp HRR peak appears with a peak heat release rate (PHRR) of 511kW/m^2, while the PHRR of PET-co-DDP and PET-co-DDP/α-ZrP nanocomposite is 400 and 270 kW/m^2, respectively. It should be noted that the PHRR of nanocomposite is only 52.8% of that of pure PET. The detailed data is shown in table 3.
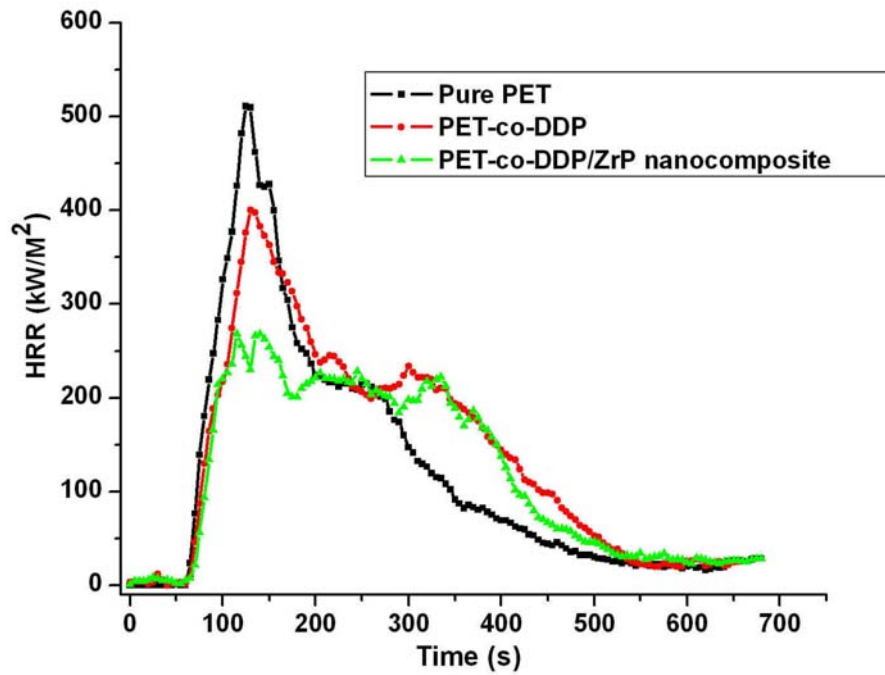
Fig. 5 Heat Release Rate (HRR) for samples

sample	TTI (s)	Av-RHR (kW/m^2)	PHRR (kW/ m^2)	TTPHR (s)	FIGRA	THR (MJ/m^2)	Residual Mass %
Pure PET	66	220	511	125	4.1	98	10
PET-co-DDP	70	172	400	150	2.7	91	21
PET-co-DDP/α -ZrP nanocomposite	73	133	270	135	2.0	76	27

TTI: time to ignition
TTPHR: time to peak heat release rate
Av: average
THR: total heat release

Table 3 Combustion parameters obtained from cone calorimeter

The samples studied also showed considerable differences in the Total Heat Release (THR/Time) curves presented in figure 6, most importantly showing that both DDP and the α-ZrP nanocomposite reduced the total amount of fuel available for combustion.
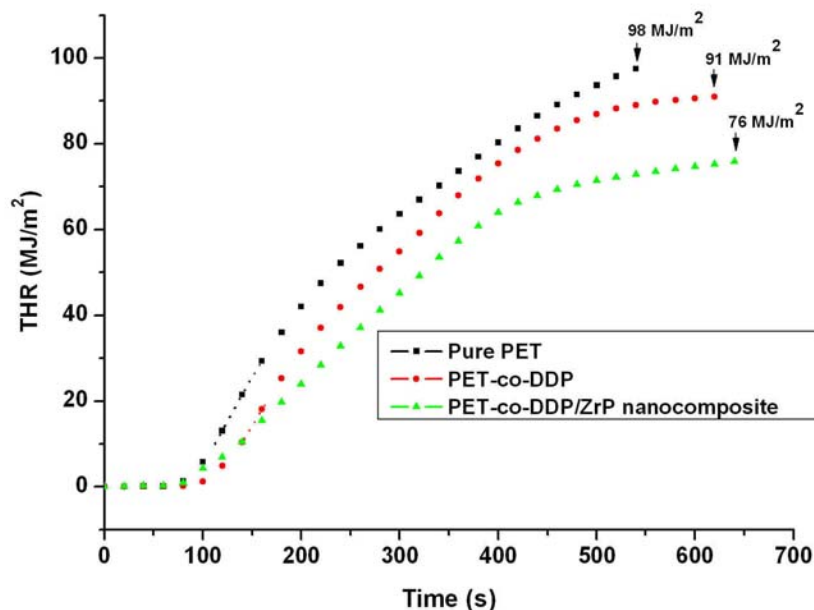
Fig. 6 Total Heat Release (THR) for samples

At the end of burning, pure PET has released a total heat of 98 MJ/m^2, the PET-co-DDP has released is 91 MJ/m^2, whereas only 76 MJ/m^2 has been released by the PET-co-DDP/α-ZrP nanocomposite. This latter significant difference results from the addition of 1% nanoparticles to the polymer, and indicates that part of the copolymer has not completely combusted, probably undergoing a partial carbonization process [32]. This is in accord with the reduced mass loss, presented in figure 7.

Figure 7 shows mass loss as a function of combustion time for pure PET, PE-co-DDP and PET-co-DDP/α-ZrP nanocomposite. The PET-co-DDP/α-ZrP nanocomposite shows a significantly lower mass loss and the higher char yields correspond to the lower THR. This indicates a condensed phase mechanism for the fire retardancy of DDP and α-ZrP. It is particularly interesting to note that this enhanced char performance was less evident in the TG experiments, but was clearly visible under the more severe conditions of the cone calorimeter at 50 kW/m^2.
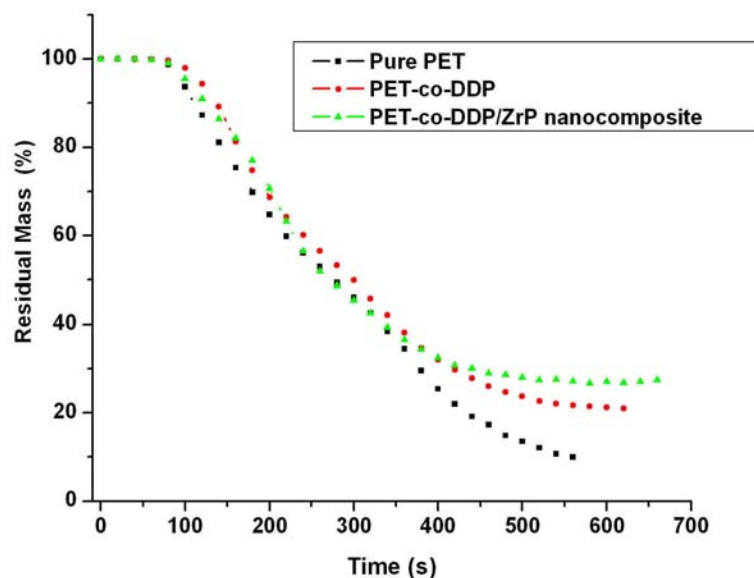
Fig. 7 Residual mass loss of the samples

One method for summarising the flammability of the fuel from the HRR curve generated by cone calorimetry is the slope of the FIGRA (fire growth rate) line, extending from the origin to the earliest, highest peak, providing an estimation of both the spread rate and the size of a fire [32], and used to estimate the contribution to fire growth of materials. FIGRA for the samples is shown in table 3. A lower value indicates a slower fire growth rate and implies lower flammability. FIGRA of PET-co-DDP/α-ZrP nanocomposite is 2, better than PET at 4.1 or PET-co-DDP at 2.7.

4. Conclusions

In this study, a novel fire retarded PET nanocomposite, PET-co-DDP/α-ZrP has been successfully prepared by direct condensation polymerisation and its thermal stability and burning behaviour have been investigated. The morphology of the nanocomposite has been investigated by XRD, SEM and TEM. The effect of small amounts of nanoparticle (α-ZrP) on the thermal stability and burning behaviour is apparent; it shows inhibition of thermal decomposition and higher char yields. From

cone calorimetry, the nanocomposite shows a very significant decrease in HRR, PHRR, THR and FIGRA compared to both the pure PET and a fire retarded PET without nanofiller. The fire retardant mechanism observed in the cone calorimeter is char formation, slowing the initial decomposition, and increasing the final char yield. In contrast to many polymer nanocomposites which show a shorter time to ignition and a lower heat release rate and peak of HRR, in this case formation of a nanocomposite increases the time to ignition, while simultaneously reducing both the PHRR and the THR. This may be related to the formation of the nanostructure which can reduce the transfer of heat and fuel in the burning process, at the same time, the metal in the nanoparticle might catalyse the reaction leading to graphitization, but this has not been demonstrated in the evidence presented here. Further work will be needed to study and understand the fire retardant mechanism and obtain more direct evidence. This study shows the potential of this approach in the development of novel halogen-free fire retardant formulations.

References:

[1] Hwang SH, Paeng SW, Kim JY, Huh W, Lee SW. Synthesis of Allylester Resin Tethered to Layered Silicates by in-situ Polymerization and Its Nanocomposite. Polym Bull 2003; 49: 329.

[2] LeBaron PC, Wang Z, Pinnavaia TJ. Polymer-layered silicate nanocomposites: an overview. Appl Clay Sci 1999; 15: 11.

[3] Wang D, Zhu J, Yao Q, Wilkie CA. A Comparison of Various Methods for the Preparation of Polystyrene and Poly(methyl methacrylate) Clay Nanocomposites. Chem Mater 2002; 14:

3837.

[4] Asrar J, Mo C. Flame retardant polyester copolymers. US Pat No. 5,399,428; 1995.

[5] Wang CS, Shich JY, Sun YM. Synthesis and properties of phosphorus containing PET and PEN(I). J Appl Polym Sci 1998; 70: 1959.

[6] Wang CS, Lin CH. Synthesis and properties of phosphorus containing PEN and PBN copolyesters. Polymer 1999; 40: 747.

[7] Wang CS, Shich JY, Sun YM. Phosphorus containing PET and PEN by direct esterification. Eur Polym J 1999; 35: 1465.

[8] Shieh JY, Wang CS. Synthesis of novel flame retardant epoxy hardeners and properties of cured products. Polymer 2001; 42: 7617.

[9] Wang YZ. Flame retardation design of PET fibers. Chengdu: Sichuan Science and Technology Press; 1994.

[10] Chen XT, Tang XD, Wang YZ. Synthesis and thermal behavior of phosphorus-containing thermotropic wholly aromatic copolyesters. Chem J Chin Univ 2002; 23: 508.

[11] Wang YZ, Chen XT, Tang XD. Synthesis, characterization and thermal properties of phosphorus-containing wholly aromatic thermotropic copolyesters. J Appl Polym Sci 2002; 86: 1278.

[12] Wang YZ, Chen XT, Tang XD, Du XH. A new approach for the simultaneous improvement of fire retardancy, tensile strength and melt dripping of poly(ethylene terephthalate). J Mater Chem 2003; 13: 1248.

[13] Wu B, Wang YZ, Wang XL, Yang KK, Jin YD, Zhao H. Kinetics of thermal oxidative degradation of phosphorus-containing flame retardant copolyester. Polym Degrad Stab 2002; 76: 401.

[14] Zhao H, Wang YZ, Wang DY, Wu B, Chen DQ, Wang XL, Yang KK. Kinetics of thermal degradation of flame retardant copolyester containing phosphorus linked pendent groups. Polym Degrad Stab 2003; 80: 135.

[15] Wang DY, Wang YZ., Wang JS, Chen DQ, Zhou Q, Yang B, Li WY. Thermal oxidative degradation behaviours of flame-retardant copolyesters containing phosphorous linked pendent group/montmorillonite nanocomposites. Polym Degrad Stab 2005, 87; 171.

[16] Wang DY, Ge XG, Wang YZ, Wang C, Qu MH, Zhou Q. A Novel Phosphorus-Containing Poly(ethylene terephthalate) Nanocomposite with Both Flame Retardancy and Anti-Dripping Effects. Macromol Mater Eng 2006; 91: 638.

[17] Zhu J, Start P, Mauritz KA, Wilkie CA. Thermal stability and flame retardancy of poly(methyl methacrylate)-clay nanocomposites. Polym Degrad Stab 2002; 77: 253.

[18] Sze´p A, Szabo´ A , Tóth N. Anna P, Marosi Gy. Role of montmorillonite in flame retardancy of ethylenevinyl acetate copolymer. Polym Degrad Stab 2006; 91: 593.

[19] Kashiwagi T, Du FM, Douglas JF, Winey KI, Harris RH, Shields JJR. Nanoparticle networks reduce the flammability of polymer nanocomposites. Nature Materials. 2005; 4: 928.

[20] Chang JH, Kim SJ. Joo YL, Im S. Poly(ethylene terephthalate) nanocomposites by in situ interlayer polymerization: the thermo-mechanical properties and morphology of the hybrid fibers. Polymer 2004; 45: 919.

[21] Ray SS, Okamoto M. Polymer/layered silicate nanocomposites: a review from preparation to processing. Prog Polym Sci 2003; 28: 1539.

[22] Clearfield A, Smith GD. Crystallography and structure of .alpha.-zirconium bis(monohydrogen orthophosphate) monohydrate. Inorg Chem 1969; 8: 431.

[23] Brandão LS, Mendes LC , Medeiros ME , Sirelli Ly, Dias ML. Thermal and mechanical properties of poly(ethylene terephthalate)/lamellar zirconium phosphate nanocomposites. J Appl Polym Sci 2006; 102: 3868.

[24] Sun L, Boo WJ, Browning RL, Sue HJ, Clearfield A. Effect of Crystallinity on the Intercalation of Monoamine in α-Zirconium Phosphate Layer Structure. Chem Mater 2005; 17: 5606.

[25] Sue HJ, Gam KT, Bestaoui N, Clearfield A, Miyamoto M, Miyatake N. Fracture behavior of α-zirconium phosphate-based epoxy nanocomposites. Acta Mater 2004; 52: 2239.

[26] Sue HJ, Gam KT, Bestaoui N, Spurr NA, Clearfield A. Epoxy Nanocomposites Based on the Synthetic α-Zirconium Phosphate Layer Structure. Chem Mater 2004; 16: 242.

[27] Boo WJ, Sun LY, Liu J, Clearfield A, Sue HJ, Mullins MJ, Pham H. Morphology and mechanical behavior of exfoliated epoxy/α-zirconium phosphate nanocomposites. Composites Science and Technology, 2007; 67: 262.

[28] Costantino U, Casciola M, Pani G, Jones DJ, Roziere J. Vibrational spectroscopic characterisation of protonic conducting polyethyleneimine-α- and γ-zirconium phosphate nanocomposites. Solid State Ionics 1997; 97: 261.

[29] Chang NJ, Chang FC. Synthesis and characterization of copolyesters containing phosphorus linked pendent groups. J Appl Polym Sci 1999; 72: 109.

[30] Price D, Liu Y, Hull TR, Milnes GJ, Kandola BK, Horrocks AR. Flame retardance of poly(methyl methacrylate) modified with phosphorus-containing compounds. Polym Degrad Stab 2002; 77: 227.

[31] Babrauskas V. SFPE Technology Report 84-10.Boston: Society of Fire Protection Engineers;

1984.

[32] EN13823: 2002 Reaction to fire tests for building products-Building products excluding
floorings exposed to the thermal attack by a single burning item.

[33] Schartel B, and Hull T R, Application of cone calorimetry to the development of materials
with improved fire performance, *Fire and Materials* 31, 327-354, (2007).

[34] Hull T R, Stec A A, Nazare S, Fire Retardant Effects of Polymer Nanocomposites, Journal
of Nanoscience and Nanotechnology (In Press, July 2008).